



Acta Universitaria

ISSN: 0188-6266

actauniversitaria@ugto.mx

Universidad de Guanajuato

México

Shulika, O. V.; Sukhoivanov, I. A.; Iakushev, S. O.; Guryev, I. V.; Andrade-Lucio, J. A.; Ibarra-Manzano, O.; Barrientos-García, A.; Ramos-Ortiz, G.

Numerical study of few-cycle pulses generation from supercontinuum in ANDi-PCF

Acta Universitaria, vol. 23, núm. 2, noviembre, 2013, pp. 40-44

Universidad de Guanajuato

Guanajuato, México

Available in: <http://www.redalyc.org/articulo.oa?id=41629563010>

- How to cite
- Complete issue
- More information about this article
- Journal's homepage in redalyc.org

redalyc.org

Scientific Information System

Network of Scientific Journals from Latin America, the Caribbean, Spain and Portugal

Non-profit academic project, developed under the open access initiative

Numerical study of few-cycle pulses generation from supercontinuum in ANDi-PCF

Estudio numérico de la generación de pulsos de algunos ciclos de un supercontinuo en una fibra de cristal fotónico con dispersión completamente normal

O. V. Shulika*, I. A. Sukhoivanov*, S. O. Iakushev**, I. V. Guryev***, J. A. Andrade-Lucio*, O. Ibarra-Manzano*, A. Barrientos-García*, G. Ramos-Ortiz****

ABSTRACT

This paper presents the design of all-normal dispersion photonic-crystal fiber optimized for pulse-preserving supercontinuum generation near 800 nm. The supercontinuum generation is analyzed numerically addressing the role of pump pulse energy and the pump wavelength deviation from the zeroth point of third-order dispersion. We have also shown that supercontinuum generated in designed ANDi-PCF from a few nanojoule 100 fs pulses can be efficiently compressed down to a sub-10-fs pulse with a simple quadratic compressor.

RESUMEN

En este trabajo se presenta el diseño de la fibra de cristal fotónico con dispersión completamente normal, optimizada para generar un supercontinuo cerca de 800 nm, preservando los pulsos. La generación del supercontinuo se analiza numéricamente considerando el papel de la desviación de la energía del pulso de bomba y su longitud de onda desde el punto cero de la dispersión de tercer orden. También, se muestra que el supercontinuo generado en la fibra diseñada usando los 100 fs pulsos de unos pocos nanojoule, se puede comprimir de manera eficiente hacia abajo a un pulso sub-10-fs con un simple compresor cuadrático.

INTRODUCTION

Generation of Supercontinuum (SC) has been a very active field of research for the last decade. A huge interest in this field was inspired by the invention of microstructured fibers and particularly photonic crystal fibers (PCFs) which allowed SC generation in a much wider range of source parameters than had been possible with bulk media or conventional fibers. Usually SC is generated in the anomalous dispersion region of optical fibers (Alfano, 2006). The broadening mechanism in this case is dominated by soliton dynamics and soliton fission, which is sensitive to input pulse fluctuations and pump laser shot noise. However, recently it was shown that all-normal dispersion photonic crystal fibers (ANDi PCFs), which exhibit convex dispersion profiles flattened near the pump wavelength, can also be used for generation of octave-spanning SC (Heidt *et al.*, 2011a). The advantages of this approach are preserving of a single pulse in the time domain, perfect temporal coherence and spectral properties suitable for efficient external recompression. Such compression has recently been demonstrated experimentally as applied to the supercontinuum generated from initial 15 fs, 1.7 nJ pulses passing through 1.7 mm long ANDi PCF. As a result, the high quality sub-two cycle pulses (5.0 fs) have been obtained (Hooper, Mosley, Muir, Wadsworth & Knight, 2011). This demonstration opens an alternative approach to the challenging problem of generating few-cycle la-

Recibido: 8 de junio de 2012
Aceptado: 14 de abril de 2013

Keywords:

Supercontinuum; photonic-crystal fibers; optical shock phenomena; pulse compression.

Palabras clave:

Supercontinuo; fibras de cristal fotónico; fenómeno de choque óptico; compresión de pulso.

* Departamento de Ingeniería Electrónica, División de Ingenierías, Campus Irapuato Salamanca. Universidad de Guanajuato. Comunidad de Palo Blanco, Carretera Salamanca-Valle de Santiago, P.O. Box 215-A, Salamanca, Gto., México. 36730. E-mail: oshulika@ugto.mx

** R&D Laboratory Photonics. Kharkiv National University of Radio Electronics. Kharkiv 61166, Ukraine.

*** Departamento de Estudios Multidisciplinarios, División de Ingenierías, Campus Irapuato Salamanca. Universidad de Guanajuato. Yuriria, Av. Universidad S/N, col. Yacatitas, Gto., México.

**** Centro de Investigaciones en Óptica, A.C. Loma del Bosque #115 Col. Lomas del Campestre, León, Gto., México. 37150.

ser pulses which are highly important in optics and spectroscopy, particularly in time-resolved studies of fundamental processes in physics, chemistry and biology (Kärtner, 2004). However, up to now the generation of the pulse-preserving SC had been demonstrated in ANDi PCFs with a dispersion flat top at 1060 nm and 650 nm (Heidt *et al.*, 2011a, 2011b). At the same time most fs-sources, at the moment, are based on the Ti: Sapphire active medium, and the typical pulse duration is about 100 fs. Here we present a simple ANDi PCF design with a flat top dispersion at 800 nm, and we analyze the generation of pulse-preserving SC in synthesized fiber applying the generalized nonlinear Schrödinger equation. We will also demonstrate that the approach of external compression of the pulse-preserving SC can be successfully expanded to the longer initial pulses up to 100 fs, which is readily available in most modern commercial ultrafast lasers.

ANDi-PCF design

Due to the complex topology of the cross section, the PCFs have to be analyzed using a numerical solution of the Helmholtz equation. Probably, the most widespread methods are finite elements and finite difference methods. However, often one can approximate the results of extensive numerical solutions well by using analytical expressions, which the framework for the right physical interpretation.

As it has turned out, the topology of ANDi PCF can be quite simple, which allows successful parametrization within classical fiber optics theory. Here, to achieve the desired properties for the synthesis of an ANDi PCF, we use the approximate method developed in (Saitoh & Koshiba, 2005). The method departs from the idea of extending the classical concept of the normalized propagation constant V to the case of PCFs. Then, it is used for the calculation of the effective index of refraction n_{eff} and the spectral dependence of dispersion. Using this method we have synthesized the ANDi PCF with solid core and hexagonal lattice, which possess characteristics presented in figure 1.

The dispersion parameter D and MFD of the designed PCF with $\Lambda = 1 \mu\text{m}$ and $d/\Lambda = 0.5$ are shown in figure 1(a). Figure 1(b) shows the dependencies of 2-nd order and 3-rd order dispersion coefficients on the wavelength. We have found that the zero third order dispersion (ZTOD) wavelength plays an important role during the generation of SC in ANDi PCF, as shown in the figure. The feature of the fiber designed is that it provides a flat top dispersion curve in the vicinity of 800 nm with $MFD = 1.59 \mu\text{m}$ and $D = -40 \text{ ps}/(\text{nm}\cdot\text{km})$ at this wavelength. It provides a nearly symmetrical

broadening of the pulse spectra that allows us to obtain SC with good properties both in spectral and time domains, as we describe in next section.

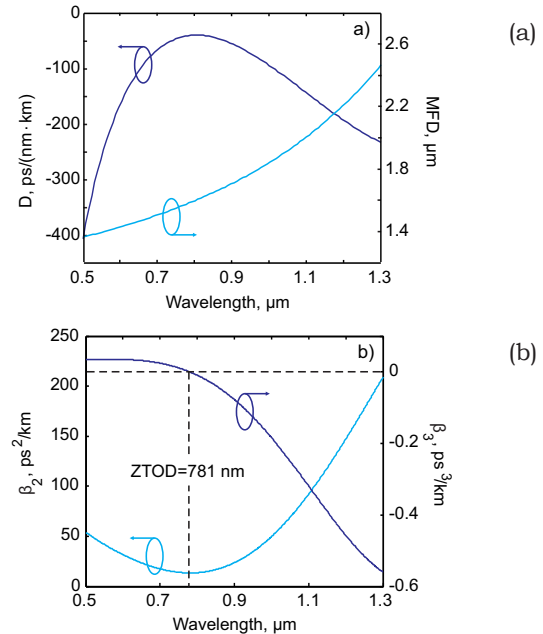


Figure 1. a) Calculated dispersion profile and MFD of ANDi PCF. b) Corresponding spectral dependencies of 2-nd order and 3-rd order dispersion coefficients.

Source: Authors own elaboration.

Supercontinuum generation and pulse compression

We simulate here pulse propagation in ANDi PCF by solving the generalized nonlinear Schrödinger equation (GNLSE) for the electric field envelope $A = (z, T)$ (Agrawal, 2001).

$$\frac{\partial A}{\partial z} = -\frac{\alpha}{2} A - \left(\sum_{n \geq 2} \beta_n \frac{i^{n-1}}{n!} \frac{\partial^n}{\partial T^n} \right) A + i\gamma \left(1 + \frac{1}{\omega_0} \frac{\partial}{\partial T} \right) \times \left((1 - f_R) |A|^2 + f_R A \int_0^\infty h_R(\tau) |A(z, T - \tau)|^2 d\tau \right), \quad (1)$$

where α is the attenuation constant, γ is the nonlinear coefficient, β_n are the dispersion coefficients obtained using a Taylor series expansion of the propagation constant $\beta(\omega)$ around the center frequency ω_0 , and $f_R = 0.18$ represents the fractional contribution of the delayed Raman response to nonlinear polarization. For the Raman response function of the silica fiber $h_R(\tau)$ the approximate analytical expression is used (Agrawal, 2001). GNLSE (2) is solved using the Runge-Kutta in the interaction picture method (Hult, 2007). During

simulations we neglect the fiber's loss because only short pieces of fiber are considered. Dispersion parameters of the designed ANDi PCF are taken up to the 8-th order, which for 800 nm are:

$$\beta_2 = 1.363 \times 10^1 \text{ ps}^2/\text{km},$$

$$\beta_3 = -8.65 \times 10^{-3} \text{ ps}^3/\text{km},$$

$$\beta_4 = 1.674 \times 10^{-4} \text{ ps}^4/\text{km},$$

$$\beta_5 = -5.48 \times 10^{-7} \text{ ps}^5/\text{km},$$

$$\beta_6 = 1.59 \times 10^{-9} \text{ ps}^6/\text{km},$$

$$\beta_7 = -3.801 \times 10^{-12} \text{ ps}^7/\text{km},$$

$$\beta_8 = 4.0 \times 10^{-15} \text{ ps}^8/\text{km}.$$

The nonlinear coefficient at 800 nm is:

$$\gamma = 113.3 \text{ 1/(W} \cdot \text{km)}.$$

For the simulation of SC generation we have chosen initial transform-limited Gaussian pulses with FWHM=100 fs at 800 nm and with different initial pulse energies. Figure 2 shows the results of simulations of SC generation carried out for various pump wavelengths λ_p . First of all, we are interested in the SC generation at the target pump wavelength 800 nm. From figure 2 we can see that the SC spectrum is quite flat for 5 nJ pump with the exception of a small dip at the pump wavelength, which becomes stronger at the 10 nJ pump. The development of this dip can be attributed to the increasing steepening of the temporal trailing pulse edge in combination with the optical wave braking-induced four wave mixing processes (Heidt, 2010). However, the most important thing is the appearance of an optical shock-type phenomenon at 16 nJ involving the development of oscillatory structure in the pulse temporal profile and in the spectrum. One can see that oscillations arise only at the trailing edge of the pulse and at the short wavelength side of the spectrum. We assume that one of following two reasons or their combined action can lead to the appearance of such an optical shock. At first, it is widely accepted that self-steepening can create an optical shock (Agrawal, 2001). Secondly, a similar asymmetrical optical shock can also arise due to the action of third order dispersion (TOD) (Iakushev, Shulika & Sukhoivanov, 2012). In any case, the most important thing is that this optical shock actually restricts the maximal energy launched to the fiber and hence the maximal width of the SC spectrum and its spectral power density.

The simulation results under shifting the pump wavelength $\lambda_p = 800 \text{ nm} \pm 10 \text{ nm}$ are shown in figure 2. We can see a rather different behavior of SC spectra.

At 810 nm, the dynamics of SC generation is very similar to that of the 800 nm pump, but the optical shock appears faster here already at 12 nJ.

At 790 nm we can see stable SC generation at least up to 35 nJ and only at 65 nJ very weak oscillations in temporal and spectral pulse profiles arise. Because the difference between the pumping wavelengths is small to induce sufficient changes of self-steepening, we assume that this different behavior resulted initially due to the influence of TOD. Indeed, the amount of TOD sufficiently changes within the 20 nm wavelength range for the designed ANDi PCF:

$$\beta_3(790 \text{ nm}) = -3.9 \times 10^{-3} \text{ ps}^3/\text{km},$$

$$\beta_3(800 \text{ nm}) = -8.65 \times 10^{-3} \text{ ps}^3/\text{km},$$

$$\beta_3(810 \text{ nm}) = -13.8 \times 10^{-3} \text{ ps}^3/\text{km}.$$

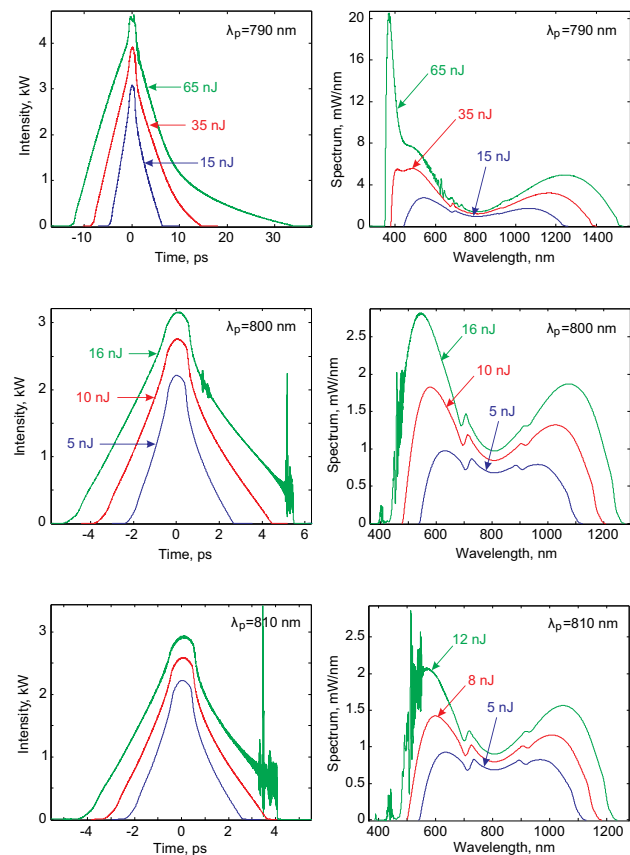


Figure 2. Supercontinuum spectra and corresponding broadened pulses at the output of the designed ANDi PCF for different pump wavelengths and initial pulse energies.

Source: Authors own elaboration.

So, one can see that the stable SC generation even a for high amount of pump energies is maintained when TOD is small. Actually, the best scenario is pumping near the ZTOD wavelength shown in the figure 1. In this case it is possible to realize a full potential of spectral broadening for the given ANDi PCF by reaching the maximal width of the SC spectrum and maximal spectral power density.

Finally, we investigated the compression of pulses at the output of ANDi PCF applying a simple quadratic compressor for compression of only a linear chirp. Figure 3 shows the results of simulations for different pump wavelengths and initial pulse energies. We considered only pulses with small and regular pulse energies in order to avoid the appearance of optical shock. The amount of group delay dispersion of compressor in each case was chosen to obtain the highest peak power of the compressed pulse, which usually corresponds to the shortest pulse duration as well.

From figure 3 we can see that maximal peak pulse powers are achieved at 790 nm where we can launch more pump energy to the fiber, whereas at 810 nm peak pulse powers are minimal. In contrast, the durations of compressed pulses at 810 nm are slightly smaller compared to those of the 790 nm and 800 nm pumps. This might be due to the stronger nonlinear chirp developed for pulses with higher initial pulse energies. Indeed, we can see that at 790 nm the uncompressed low-level pedestal in the pulse shape is stronger compared to those of the 800 nm and 810 nm pumps. Therefore, we believe that the application of more sophisticated compression techniques for elimination of nonlinear chirp is also desired in order to exploit the huge spectral bandwidth of SC spectra generated at high pump energies fully. We think that the application of, for instance, dispersive mirrors (Pervak, Ahmad, Fulop, Trubetskov & Tikhonravov, 2009) will allow obtaining even shorter pulses available for a given spectral bandwidth.

CONCLUSIONS

To conclude, we have proposed an all-normal dispersion photonic-crystal fiber optimized for pumping at 800 nm. We have shown numerically that octave-spanning supercontinuum generation is readily reachable applying 10 cm of this fiber and a few nJ 100 fs pulses at 800 nm. However, we have found that optical shock appears at higher pump pulse energies and it actually restricts the maximal width of SC spectrum. The main reason for the development of this optical shock is the

influence of third order dispersion. The strength of this shock sufficiently depends on the pump wavelength. We found that the best scenario is pumping near the ZTOD wavelength. In this case it is possible to realize a full potential of spectral broadening for a given ANDi PCF by reaching the maximal width of SC spectrum and the maximal spectral power density. We have also shown that SC generated in the designed ANDi PCF can be efficiently compressed down to 8-fs pulse applying a simple quadratic compressor. The maximal peak power of compressed pulses can be achieved also near the ZTOD. However, for higher initial pump pulse energies the uncompressed low level pedestal in the pulse shape becomes stronger, and hence the application of more sophisticated compression techniques is desired in order to achieve the shortest pulses available for generated SC spectra.

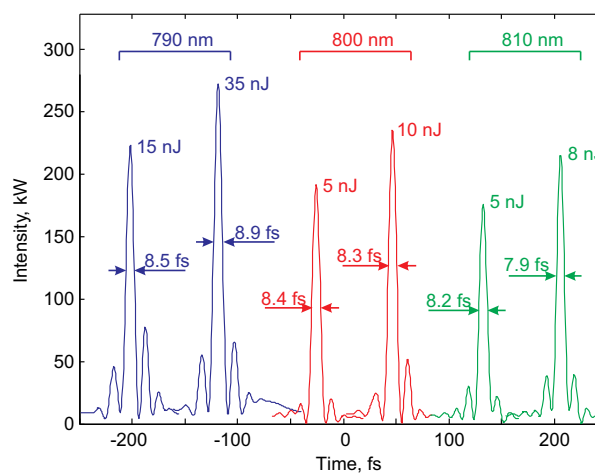


Figure 3. Compressed pulses for different pump wavelengths and initial pulse energies.

Source: Authors own elaboration.

ACKNOWLEDGEMENTS

This work is partially supported by SEP/PROMEP (project UGTO-PTC-371), *Consejo nacional de Ciencia y Tecnología* (Conacyt) (project 175573/12), and University of Guanajuato (projects DAIP-334/13 and DAIP-192/13).

REFERENCES

- Agrawal, G. P. (2001). *Nonlinear Fiber Optics* (3rd ed.). San Diego: Academic Press.
- Alfano, R. R. (2006). *The Supercontinuum Laser Source* (2nd ed.). New York: Springer-Verlag.

- Heidt, A. M. (2010). Pulse preserving flat-top supercontinuum generation in all-normal dispersion photonic crystal fibers. *Journal Optical Society of America B*, 27(3), 550-559.
- Heidt, A. M., Hartung, A., Bosman, G. W., Krok, P., Rohwer, E. G., Schwoerer, H. & Bartelt, H. (2011). Coherent octave spanning near-infrared and visible supercontinuum generation in all-normal dispersion photonic crystal fibers. *Optics Express*, 19(4), 3775-3787.
- Heidt, A. M., Rothhardt, J., Hartung, A., Bartelt, H., Rohwer, E., Limpert, J. & Tünnermann, A. (2011). High quality sub-two cycle pulses from compression of supercontinuum generated in all-normal dispersion photonic crystal fiber. *Optics Express*, 19(15), 13 873-13 879.
- Hooper, L. E., Mosley, P. J., Muir, A. C., Wadsworth, W. J. & Knight, J. C. (2011). Coherent supercontinuum generation in photonic crystal fiber with all-normal group velocity dispersion. *Optics Express*, 19(6), 4902-4907.
- Hult, J. (2007). A fourth-order runge-kutta in the interaction picture method for simulating supercontinuum generation in optical fibers. *Journal Lightwave Technology*, 25(12), 3770 -3775.
- Iakushev, S. O., Shulika, O. V. & Sukhoivanov, I. A. (2012). Passive nonlinear reshaping towards parabolic pulses in the steady-state regime in optical fibers. *Optics Communications*, 285, 4493-4499.
- Kärtner, F. X. (2004). *Few-cycle Laser Pulse Generation and its Applications*. Berlin: Springer-Verlag.
- Pervak, V., Ahmad, I., Fulop, J., Trubetskov, M. K. & Tikhonravov, A. V. (2009). Comparison of dispersive mirrors based on the time-domain and conventional approaches, for sub-5-fs pulses. *Optics Express*, 17(4), 2207-2217.
- Saitoh, K. & Koshiba, M. (2005). Empirical relations for simple design of photonic crystal fibers. *Optics Express*, 13(1), 267-274.